The Characterisation and Manipulation of Novel Topological Phases of Matter

James de Lisle

Department of Physics and Astronomy

University of Leeds

A thesis submitted for the degree of

Doctor of Philosophy

30th January 3000

This thesis is dedicated to...

Acknowledgements

My thanks to...

Abstract

My abstract in here...

Abbreviations

k_B	Boltzmann's constant
k_BT	Thermal energy
...	...

Contents

List of Figures

Chapter 1

Introduction

1.1 Introduction

Defining and distinguishing phases of matter has been a continuing effort by physicists for many years.

1.2 1D Topological Superconductor

In order to illustrate the essential elements of a topological condensed matter system, we now present a construction and analysis of the simplest superconducting lattice model, the Kitaev wire [1].

1.2.1 Dirac fermions

Given $N \in \mathbb{N}^+$ Dirac fermions, hereby denoted simply as fermions, they can be represented by a set of second quantised fermionic field operators $\{a_j\}$ and their conjugate partners $\{a_j^\dagger\}$, where $j = 1, ..., N$. They obey the following commutation relations

$$\{a_i, a_j^\dagger\} = \delta_{ij} \qquad \{a_i^{(\dagger)}, a_j^{(\dagger)}\} = 0 \tag{1.1}$$

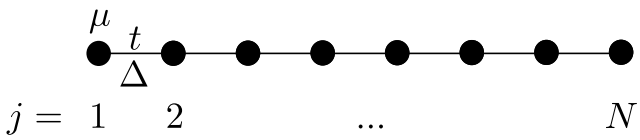

Figure 1.1: A schematic representation of the Kitaev 1D wire. A set of N sites denoted by the black dots and indexed by $j = 1, .., N$ are connected by black lines. To each site we associate a fermion a_j to which we associate a chemical potential $\mu \in \mathbb{R}$. We allow for fermions to tunnel to adjacent sites with amplitude $t \in \mathbb{R}$ and pair with adjacent fermions with amplitude $\Delta \in \mathbb{R}$

where δ_{ij} Kronercker delta function. These operators act on a tensor product of Fock states. A general state of the fermionic system, $|\psi\rangle$ can be written as

$$|\psi\rangle = \sum_{n_i=0,1} \left(\alpha_{n_1,\ldots,n_N} \bigotimes_{i=1}^{N} |n_i\rangle \right), \tag{1.2}$$

where $\alpha_{n_1,\ldots,n_N} \in \mathbb{C}$ and

$$\bigotimes_{j=1}^{N} |n_j\rangle = \left(\bigotimes_{j=1}^{N} \left(a_j^\dagger\right)^{n_j} \right) \left(\bigotimes_{j=1}^{N} |0\rangle \right). \tag{1.3}$$

1.2.2 Real space tight-binding model

We take a chain of N sites indexed by $j = 1, ..., N$ and to each site we associate a fermion a_j. To each fermion we associate the same chemical potential μ and we allow for nearest neighbour tunnelling and pairing with amplitudes t and Δ respectively, with $\mu, t, \Delta \in \mathbb{R}$. This arrangement is shown in fig. 1.1. With this information we can write down a tight binding Hamiltonian

$$H = \sum_{j=1}^{N} \left(\mu a_j^\dagger a_j - \frac{1}{2} + t a_j^\dagger a_{j+1} + \Delta a_j a_{j+1} \right) + h.c., \tag{1.4}$$

where $h.c.$ denotes the Hermitian conjugate. We have chosen periodic boundary conditions such that $N + 1$ is 1.

1.2.3 Momentum space and the Fourier tansform

Because (1.4) is translationally invariant and has preiodic boundary conditions, we can transform it into momentum space via the Fourier transform. The transformation is defined as

$$a_j = \sum_p e^{ipj} a_p \qquad\qquad a_j^\dagger = \sum_p e^{-ipj} a_p^\dagger, \tag{1.5}$$

where $p \in [-\pi, \pi)$, also called the Brillouin zone (BZ). The transformed Hamiltonian is written as

$$H = \sum_p \big(\mu + t\cos(p)\big)\Big(a_p^\dagger a_p - a_{-p} a_{-p}^\dagger\Big) + i\Delta\sin(p)\Big(a_p a_{-p} - a_{-p}^\dagger a_p^\dagger\Big). \tag{1.6}$$

We can now write the Hamiltonian in Bogoliubov-de Gennes form

$$H = \sum_p \boldsymbol{\psi}_p^\dagger h(\boldsymbol{\lambda}, p)\boldsymbol{\psi}_p, \tag{1.7}$$

where $\boldsymbol{\psi}_p = \begin{pmatrix} a_p & a_{-p}^\dagger \end{pmatrix}^{\mathrm{T}}$, $\boldsymbol{\lambda} = \begin{pmatrix} \mu & \Delta & t \end{pmatrix}$, and $h(p)$ is a 2×2 Hermitian matrix given by

$$h(p) = \begin{pmatrix} \epsilon(p) & \Xi(p) \\ \Xi^*(p) & -\epsilon(p) \end{pmatrix} \tag{1.8}$$

where $\epsilon(\mu, t, p) = \mu + t\cos(p)$ and $\Xi(\Delta, p) = i\Delta\sin(p)$. We shall call $h(\boldsymbol{\lambda}, p)$ the *kernel Hamiltonian*. From the kernal Hamiltonian we can extract many useful quantities such as the energy spectrum and the model's topological invariant, the winding number.

1.2.4 Symmetries

Free fermionic models can be classified by the symmetries of the kernel Hamiltonian [2, 3, 4]. The presence (or not) of time-reversal (TR), particle-hole (PH) and sublattice (S) symmetries determines which of 10 classes a given Hamiltonian is in. More shall be said of the so called 10-fold way later in this document.

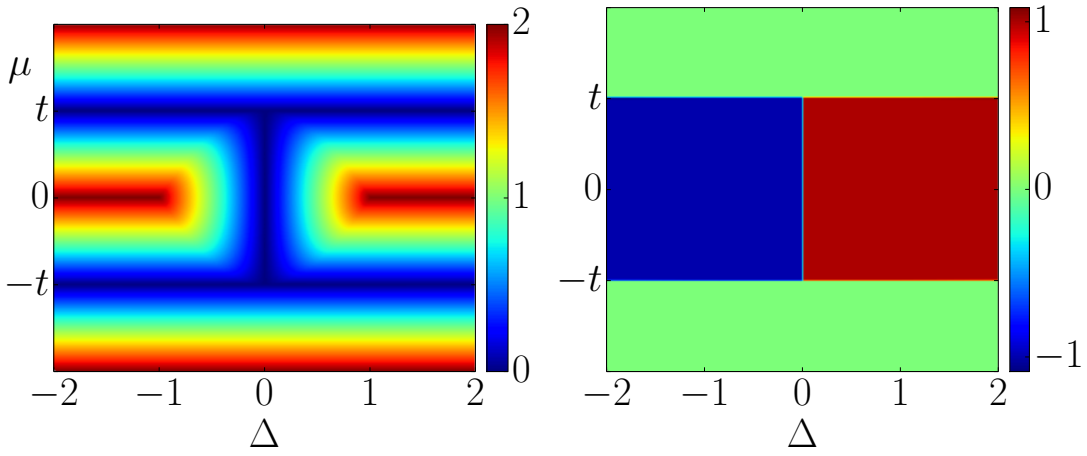

Figure 1.2: (Left) The energy gap, ΔE of the Kitaev wire as a function of the chemical potential, μ, and the superconducting order parameter Δ. The data was obtained via exact diagonalisation of (1.8). (Right) The winding number, ν_{1D}, of the Kitaev wire. Each gapped phase is separated by a gappless line as depicted in the diagram of the gap on the left. The data was obtained via numerical evaluation of (1.12).

The model as it stands obeys both TR and PH symmetries and by implication S symmetry.

1.2.5 Energy Spectrum and ground state

The model supports a pair of eigenvalues and eigenvectors, $E^{\pm}(\boldsymbol{\lambda}, p)$ and $|\psi_{\pm}(\boldsymbol{\lambda}, p)\rangle$. As the model is PH symmetric the spectrum will be symmetric about zero energy. This is confirmed when we look at the analytic expression for the eigenvalues of (1.8),

$$E^{\pm}(\boldsymbol{\lambda}, p) = \pm\sqrt{|\epsilon(\mu, t, p)|^2 + |\Xi(\Delta, p)|^2}. \tag{1.9}$$

We define the *energy gap*, denoted $\Delta E(\boldsymbol{\lambda})$, as

$$\Delta E(\boldsymbol{\lambda}) = 2 \cdot \min_p |E^{+}(\boldsymbol{\lambda}, p)|. \tag{1.10}$$

In fig. 1.2 (left) we plot $\Delta E(\boldsymbol{\lambda})$ as a function of μ and Δ. The diagram is separated into four regions where $\Delta E(\boldsymbol{\lambda}) \neq 0$ which are separated by lines where

$\Delta E(\boldsymbol{\lambda}) = 0$.

We take the system to be at half filling. This means that all of the negative energy states are occupied and the ground state is state associated with $E^-(p)$, $|\psi_{gs}(p)\rangle = |\psi_-(p)\rangle$.

1.2.6 Winding number

The topological phase of the system is determined by the winding number, $\nu_{1\mathrm{D}}$. In order to define $\nu_{1\mathrm{D}}$ we must first define a unit vector $\hat{\boldsymbol{s}}(p)$ which parametrises the kernel Hamiltonian

$$h(\boldsymbol{\lambda}, p) = \boldsymbol{s}(\boldsymbol{\lambda}, p) \cdot \boldsymbol{\sigma} = |\boldsymbol{s}(\boldsymbol{\lambda}, p)| \hat{\boldsymbol{s}}(\boldsymbol{\lambda}, p) \cdot \boldsymbol{\sigma} \tag{1.11}$$

where $\boldsymbol{\sigma} = \begin{pmatrix} \sigma^x & \sigma^y & \sigma^z \end{pmatrix}^{\mathrm{T}}$ and $\hat{\boldsymbol{s}}(\boldsymbol{\lambda}, p) : T^1 \to S^2$. The vector $\hat{\boldsymbol{s}}(\boldsymbol{\lambda}, p)$ is a map between the 1D-torus that is the Brillouin zone and the unit two sphere. We define $\nu_{1\mathrm{D}} : \mathbb{R}^3 \to \mathbb{Z}$ as

$$\nu_{1\mathrm{D}}(\boldsymbol{\lambda}) = \int_{\mathrm{BZ}} dp \;\; \boldsymbol{\theta}(\boldsymbol{\lambda}, p) \cdot \hat{\boldsymbol{u}}_\perp(\boldsymbol{\lambda}, p), \tag{1.12}$$

where $\boldsymbol{\theta}(\boldsymbol{\lambda}, p) = \big(\hat{\boldsymbol{s}}(\boldsymbol{\lambda}, p) \times \partial_p \hat{\boldsymbol{s}}(\boldsymbol{\lambda}, p)\big)$ and $(\hat{\boldsymbol{u}}_\perp(\boldsymbol{\lambda}, p))_i = |\theta_i(\boldsymbol{\lambda}, p)|/|\boldsymbol{\theta}(\boldsymbol{\lambda}, p)|$. The integral (1.12) counts the number of times the vector $\hat{\boldsymbol{s}}(\boldsymbol{\lambda}, p)$ winds around S^2. Fig. 1.2 (right) depicts the winding number for the Kitaev wire as a function of μ and Δ. There are two distinct topological phases with $\nu = \pm 1$ and two separated trivial phases with $\nu = 0$. The winding number is invariant within each gapped phase, only changing value when $\Delta E(\boldsymbol{\lambda}) \to 0$. This can be understood by looking at the definition of $\hat{\boldsymbol{s}}(\boldsymbol{\lambda}, p)$. It is easy to show that $|\boldsymbol{s}(\boldsymbol{\lambda}, p)| = E^{\pm}(\boldsymbol{\lambda}, p)$. Therefore when $\Delta E(\boldsymbol{\lambda}) \to 0$, $\hat{\boldsymbol{s}}(\boldsymbol{\lambda}, p)$ becomes undefined. This discontinuity in $\nu_{1\mathrm{D}}(\boldsymbol{\lambda})$ allows the invariant to change value.

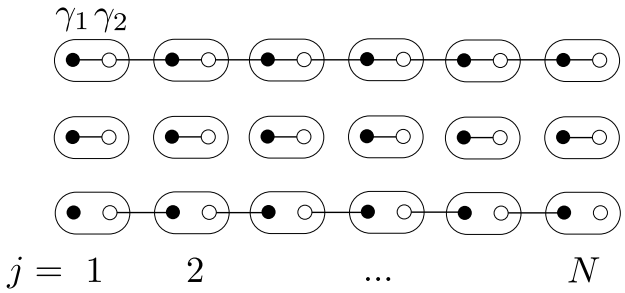

Figure 1.3: (Top) The Kitaev chain drawn in the Majorana basis. Each site j supports two Majorana fermions $\gamma_{1,j}$ and $\gamma_{2,j}$. (Middle) The Majorana chain with $\mu > 0$ and $\Delta = t = 0$, leading to the Majoranas on the same site being paired together. This point in parameter space is in the trivial phase with $\nu_{1\mathrm{D}}(\boldsymbol{\lambda}) = 0$. (Bottom) The Majorana chain with $\mu = 0$ and $\Delta = t > 0$, leading to Majoranas on adjacent sites being paired together. Due to the open boundary conditions, there are unpaired Majorana fermions at each end of the wire.

1.2.7 Majorana fermions and edge states

A natural basis for describing topological superconductors is the Majorana basis. It is related to the Dirac fermion basis in the following way

$$a_j = \frac{\gamma_{1,j} + i\gamma_{2,j}}{2} \qquad\qquad a_j^\dagger = \frac{\gamma_{1,j} - i\gamma_{2,j}}{2} \tag{1.13}$$

where $\gamma_{\alpha,j}$ are the Majorana operators. They have the singular property that they are self dual, i.e. $\gamma_{\alpha,j} = \gamma_{\alpha,j}^\dagger$, and they obey the following commutation relations

$$\left\{\gamma_{\alpha,i}, \gamma_{\beta,j}\right\} = 2\delta_{\alpha\beta}\delta_{ij}, \tag{1.14}$$

implying that $\gamma_{\alpha,j}^2 = 1$. We can rewrite (1.4) in the Majorana basis to get

$$H = \frac{i}{2}\sum_{j=1}^{N}\Big[\mu\gamma_{1,j}\gamma_{2,j} + \big(t+\Delta\big)\gamma_{2,j}\gamma_{1,j+1} + \big(-t+\Delta\big)\gamma_{1,j}\gamma_{2,j+1}\Big]. \tag{1.15}$$

Through judicious choices of μ, Δ and t we can eliminate different terms in (1.15). These different choices of the coupling configuration are shown in fig. 1.3. If we

pick a point in parameter space that is in the trivial phase, as depicted in fig. 1.2, such as $\mu > 0$ and $\Delta = t = 0$ then (1.15) becomes $H = \frac{i}{2}\sum_j \mu\gamma_{1,j}\gamma_{2,j}$ and the configuration becomes that of fig. 1.3 (middle). However if we pick a point in the non-trivial phase, such as $\mu = 0$ and $\Delta = t > 0$, then (1.15) becomes $H = it\sum_j \gamma_{2,j}\gamma_{1,j+1}$ and as depicted in fig. 1.3 (bottom) we are left with two unpaired Majorana fermions, one at each end of the chain. These two Majoranas do not appear in the modified Hamiltonian.

Chapter 2

Decomposition of the Chern Number in 2D Systems

In this chapter we will address the problem of the measurement of the Chern number in two component systems [5]. In section 2.1 we review the definitions and conventions associated with the Chern number and winding number of single species systems in two spatial dimensions.

2.1 Chern number and winding numbers in two spatial dimensions

The following analysis stands in both the superconducting and insulating cases, despite the derivation being slightly different. Where necessary, we present here the definitions and derivations in the context of insulating systems, and the superconducting case will be addressed separately. Translationally invariant lattice models in two spatial dimensions supporting $N = 2$ species of fermion $a_{\alpha,\boldsymbol{p}}$, with $\alpha = 1, 2$, can be written in the form []

$$H = \sum_{p} \boldsymbol{\psi}^{\dagger}_{\boldsymbol{p}} h(\boldsymbol{\lambda}, \boldsymbol{p}) \boldsymbol{\psi}_{\boldsymbol{p}}, \tag{2.1}$$

where $\boldsymbol{\psi}_{\boldsymbol{p}} = \begin{pmatrix} a_{1,\boldsymbol{p}} & a_{2,\boldsymbol{p}} \end{pmatrix}^{\mathrm{T}}$ and $\boldsymbol{p} = \begin{pmatrix} p_x, & p_y \end{pmatrix} \in \mathrm{BZ}$ where BZ is the Brillouin zone. $h(\boldsymbol{\lambda}, \boldsymbol{p})$ is an 2×2 Hermitian matrix called the *kernel Hamiltonian* where $\boldsymbol{\lambda} = \begin{pmatrix} \lambda_1, & \dots, & \lambda_M \end{pmatrix} \in \mathcal{M}^M$ such that $\mathcal{M}^M$ is in general an M-dimensional complex manifold we call *parameter space*. The ground state of the system is given by $|\Psi\rangle = \prod_{\boldsymbol{p}} |\psi_{\boldsymbol{p}}\rangle$, which is defined in terms of the operators $a^{\dagger}_{\alpha,\boldsymbol{p}}$ acting on the fermionic vacuum $|0\rangle \otimes |0\rangle$. The kernel Hamiltonian has a pair of eigenvectors, $|\psi^{\pm}(\boldsymbol{\lambda}, \boldsymbol{p})\rangle$, and eigenvalues, $E^{\pm}(\boldsymbol{\lambda}, \boldsymbol{p})$. Because the model is particle-hole symmetric, the spectrum is symmetric about zero energy. We take the system to be at *half filling* by which we mean we make the ground state of the system by filling up the negative energy states so that the ground state of $h(\boldsymbol{\lambda}, \boldsymbol{p})$ is $|\psi^{-}(\boldsymbol{\lambda}, \boldsymbol{p})\rangle$. The Chern number, $\nu \in \mathbb{Z}$, that characterises the topological phase of the system is defined as

$$\nu_{2\mathrm{D}}(\boldsymbol{\lambda}) = -\frac{i}{2\pi} \int_{\mathrm{BZ}} d^2p \ \mathrm{tr}\Big(P_{\boldsymbol{\lambda},\boldsymbol{p}} \big[\partial_{p_x} P_{\boldsymbol{\lambda},\boldsymbol{p}}, \partial_{p_y} P_{\boldsymbol{\lambda},\boldsymbol{p}} \big] \Big) \tag{2.2}$$

where $P_{\boldsymbol{\lambda},\boldsymbol{p}} = |\psi^{-}(\boldsymbol{\lambda}, \boldsymbol{p})\rangle \langle \psi^{-}(\boldsymbol{\lambda}, \boldsymbol{p})|$ is the projector on the ground state of $h(\boldsymbol{\lambda}, \boldsymbol{p})$. This is not the only way we can write the Chern number.

2.1.1 The Berry phase representation of $\nu_{2\mathrm{D}}$

The Chern number can also be written in terms of the Berry phase accrued around the boundary of the BZ. To see this we take the projector definition of the Chern number (2.2) and substitute in the definition of the projector $P_{\boldsymbol{\lambda},\boldsymbol{p}}$

$$\begin{aligned} \nu_{2\mathrm{D}}(\boldsymbol{\lambda}) = -\frac{i}{2\pi} \int_{\mathrm{BZ}} d^2p \ \langle \psi^{-}(\boldsymbol{\lambda}, \boldsymbol{p})| \Big[& |\partial_{p_x} \psi^{-}(\boldsymbol{\lambda}, \boldsymbol{p})\rangle \langle \psi^{-}(\boldsymbol{\lambda}, \boldsymbol{p})| \\ & + |\psi^{-}(\boldsymbol{\lambda}, \boldsymbol{p})\rangle \langle \partial_{p_x} \psi^{-}(\boldsymbol{\lambda}, \boldsymbol{p})| \, , |\partial_{p_y} \psi^{-}(\boldsymbol{\lambda}, \boldsymbol{p})\rangle \langle \psi^{-}(\boldsymbol{\lambda}, \boldsymbol{p})| \\ & + |\psi^{-}(\boldsymbol{\lambda}, \boldsymbol{p})\rangle \langle \partial_{p_x} \psi^{-}(\boldsymbol{\lambda}, \boldsymbol{p})| \Big] \, |\psi^{-}(\boldsymbol{\lambda}, \boldsymbol{p})\rangle \, . \end{aligned} \tag{2.3}$$

$|\psi^-(\boldsymbol{\lambda},\boldsymbol{p})\rangle$ is normalised and therefore $\partial_\mu \langle\psi^-(\boldsymbol{\lambda},\boldsymbol{p})|\psi^-(\boldsymbol{\lambda},\boldsymbol{p})\rangle = 0$, with $\mu = p_x, p_y$, such that

$$\langle\partial_\mu\psi^-(\boldsymbol{\lambda},\boldsymbol{p})|\psi^-(\boldsymbol{\lambda},\boldsymbol{p})\rangle = -\langle\psi^-(\boldsymbol{\lambda},\boldsymbol{p})|\partial_\mu\psi^-(\boldsymbol{\lambda},\boldsymbol{p})\rangle\,. \tag{2.4}$$

By expanding (2.3) and applying (2.4) we have

$$\nu_{2\mathrm{D}}(\boldsymbol{\lambda}) = -\frac{i}{2\pi}\int_{\mathrm{BZ}} d^2p\ \ \varepsilon_{\mu\nu}\langle\partial_{p_\mu}\psi^-(\boldsymbol{\lambda},\boldsymbol{p})|\partial_{p_\nu}\psi^-(\boldsymbol{\lambda},\boldsymbol{p})\rangle\,. \tag{2.5}$$

We recognise that the integrand of (2.5) is the Berry curvature $F(\boldsymbol{\lambda},\boldsymbol{p})$

$$F(\boldsymbol{\lambda},\boldsymbol{p}) = \varepsilon_{\mu\nu}\partial_\mu A_\nu = \varepsilon_{\mu\nu}\langle\partial_{p_\mu}\psi^-(\boldsymbol{\lambda},\boldsymbol{p})|\partial_{p_\nu}\psi^-(\boldsymbol{\lambda},\boldsymbol{p})\rangle\,, \tag{2.6}$$

where $\boldsymbol{A} = \langle\psi^-(\boldsymbol{\lambda},\boldsymbol{p})|\boldsymbol{\partial}|\psi^-(\boldsymbol{\lambda},\boldsymbol{p})\rangle$ with $\boldsymbol{\partial} = \begin{pmatrix}\partial_{p_x}, & \partial_{p_y}\end{pmatrix}$. Using Stokes' theorem we can write the Chern number as

$$\nu_{2\mathrm{D}}(\boldsymbol{\lambda}) = -\frac{i}{2\pi}\int_{\mathrm{BZ}} d^2p\ \ F(\boldsymbol{\lambda},\boldsymbol{p}) = -\frac{i}{2\pi}\oint_{\partial\mathrm{BZ}} d\boldsymbol{p}\cdot\boldsymbol{A}, \tag{2.7}$$

where ∂BZ is the boundary of the Brillouin zone.

2.1.2 The winding number representation of $\nu_{2\mathrm{D}}$

Under the constraint that $\dim[h(\boldsymbol{p})] = 2$ it can be parametrised in terms of a normalised vector $\hat{\boldsymbol{s}}(\boldsymbol{\lambda},\boldsymbol{p}) : \mathrm{BZ} \to S^2$

$$h(\boldsymbol{\lambda},\boldsymbol{p}) = |\boldsymbol{s}(\boldsymbol{\lambda},\boldsymbol{p})|\hat{\boldsymbol{s}}(\boldsymbol{\lambda},\boldsymbol{p})\cdot\boldsymbol{\sigma}, \tag{2.8}$$

where $\boldsymbol{\sigma} = \begin{pmatrix}\sigma^x, & \sigma^y, & \sigma^z\end{pmatrix}$. We can express $\nu_{2\mathrm{D}}(\boldsymbol{\lambda})$ as the winding of $\hat{\boldsymbol{s}}(\boldsymbol{\lambda},\boldsymbol{p})$ over BZ. Using (2.8) we can write the projector $P_{\boldsymbol{\lambda},\boldsymbol{p}}$ as

$$P_{\boldsymbol{\lambda},\boldsymbol{p}} = \frac{1}{2}\big(\mathbb{I} - \hat{\boldsymbol{s}}(\boldsymbol{\lambda},\boldsymbol{p})\cdot\boldsymbol{\sigma}\big), \tag{2.9}$$

where $\mathbb{I}$ is the identity matrix. By substituting (2.9) into (2.2) and employing the identities

$$\big(\boldsymbol{a}\cdot\boldsymbol{\sigma}\big)\big(\boldsymbol{b}\cdot\boldsymbol{\sigma}\big) = \mathbb{I}\boldsymbol{a}\cdot\boldsymbol{b} + i\boldsymbol{\sigma}\cdot\boldsymbol{a}\times\boldsymbol{b} \tag{2.10}$$

for two 3-vectors $\boldsymbol{a}$ and $\boldsymbol{b}$, and

$$\mathrm{tr}\big(\sigma^\alpha\sigma^\beta\big) = 2\delta_{\alpha\beta}; \qquad \alpha,\beta = x,y,z, \tag{2.11}$$

we have

$$\begin{aligned}\nu_{\mathrm{2D}}(\boldsymbol{\lambda}) =& -\frac{i}{2\pi}\int_{\mathrm{BZ}} d^2p\ \ \mathrm{tr}\Big(\,|\psi^-(\boldsymbol{\lambda},\boldsymbol{p})\rangle\,\langle\psi^-(\boldsymbol{\lambda},\boldsymbol{p})|\,\frac{1}{4}\big[\partial_{p_x}\hat{\boldsymbol{s}}(\boldsymbol{\lambda},\boldsymbol{p})\cdot\boldsymbol{\sigma},\partial_{p_y}\hat{\boldsymbol{s}}(\boldsymbol{\lambda},\boldsymbol{p})\cdot\boldsymbol{\sigma}\big]\Big)\\ =&\frac{1}{4\pi}\int_{\mathrm{BZ}} d^2p\ \ \hat{\boldsymbol{s}}(\boldsymbol{\lambda},\boldsymbol{p})\cdot\big(\partial_{p_x}\hat{\boldsymbol{s}}(\boldsymbol{\lambda},\boldsymbol{p})\times\partial_{p_x}\hat{\boldsymbol{s}}(\boldsymbol{\lambda},\boldsymbol{p})\big)\\ \equiv&\tilde{\nu}_{\mathrm{2D}}(\boldsymbol{\lambda})\end{aligned} \tag{2.12}$$

As the BZ is spanned, $\hat{\boldsymbol{s}}(\boldsymbol{\lambda},\boldsymbol{p})$ winds around the sphere S^2 an integer number of times. If $\nu_{\mathrm{2D}}(\boldsymbol{\lambda}) \neq 0$ we say that the system is in a topological phase.

There also exists a direct link between the winding number (2.12) and Berry phase (2.7) represenations which is shown in appendix **??**.

2.1.3 Observability of the winding number

The winding number is of particular interest as it is directly observable. It is easy to show that

$$\hat{\boldsymbol{s}}(\boldsymbol{\lambda},\boldsymbol{p}) = \langle\psi^-(\boldsymbol{\lambda},\boldsymbol{p})|\boldsymbol{\sigma}|\psi^-(\boldsymbol{\lambda},\boldsymbol{p})\rangle = \langle\psi_{\boldsymbol{p}}|\boldsymbol{\Sigma}|\psi_{\boldsymbol{p}}\rangle \tag{2.13}$$

where $\boldsymbol{\Sigma} = \boldsymbol{\psi}^\dagger_{\boldsymbol{p}}\boldsymbol{\sigma}\boldsymbol{\psi}_{\boldsymbol{p}}$ are the second quantised representations of the Pauli operators explicitly given by

$$\begin{aligned}\Sigma^x =& a^\dagger_{1,\boldsymbol{p}}a_{2,\boldsymbol{p}} + a^\dagger_{2,\boldsymbol{p}}a_{1,\boldsymbol{p}},\\ \Sigma^y =& -ia^\dagger_{1,\boldsymbol{p}}a_{2,\boldsymbol{p}} + ia^\dagger_{2,\boldsymbol{p}}a_{1,\boldsymbol{p}},\\ \Sigma^z =& a^\dagger_{1,\boldsymbol{p}}a_{1,\boldsymbol{p}} - a^\dagger_{2,\boldsymbol{p}}a_{2,\boldsymbol{p}}\end{aligned} \tag{2.14}$$

In systems of cold atom systems, by studying how the cloud of atoms expands when the trap is switched off, one can obtain a set of time of flight images from

which one can extract the expectation values of the operators $a^\dagger_{\boldsymbol{p}} a_{\boldsymbol{p}}$ and $b^\dagger_{\boldsymbol{p}} b_{\boldsymbol{p}}$. As such the σ^z component of (2.13) can be measured and the $\sigma^{x,y}$ components can be obtained through suitable rotations.

2.1.4 Breakdown of the winding number representation

If the number of species of fermion in the system $N > 2$ then $h(\boldsymbol{\lambda}, \boldsymbol{p})$ can no longer be expanded in the Pauli basis. We can choose to expand it in terms of some higher dimensional basis of matrices, then however $\dim[\hat{\boldsymbol{s}}(\boldsymbol{\lambda}, \boldsymbol{p})] > 3$ and the derivation of the winding number in sec. 2.1.2 is no longer sound. While it would, in principle, be possible to construct the components of some higher dimensional $\hat{\boldsymbol{s}}(\boldsymbol{\lambda}, \boldsymbol{p})$ from time of flight images, we no longer know how to reconstruct the Chern number from them.

2.2 Decomposition of the Chern number into subsystem winding numbers

We now present the analytic argument for decomposing the Chern number as a sum of winding numbers associated with each subsystem. We present first present the argument for topological insulators that preserve particle number and then show that it also holds for parity conserving topological superconductors.

2.2.1 Derivation for topological insulators

Consider a system with four different species of fermion a_1, a_2, b_1, and b_2 where the a/b bi-partition can correspond to a number of different physical distinctions (e.g. spin degrees of freedom, atomic levels, different sectors of some discrete symmetry). Assuming translational invariance and periodic boundary conditions

we can write the Hamiltonian as (2.1) with $\boldsymbol{\psi}_{\boldsymbol{p}} = \begin{pmatrix} a_{1,\boldsymbol{p}} & a_{2,\boldsymbol{p}} & b_{1,\boldsymbol{p}} & b_{2,\boldsymbol{p}} \end{pmatrix}^{\mathrm{T}}$. A general state in the Hilbert space of the system can be written as

$$|\Psi\rangle = \prod_{\boldsymbol{p}} \left(\sum_{n^j_{i,\boldsymbol{p}}=0,1} \alpha_{n^a_{1,\boldsymbol{p}},n^a_{2,\boldsymbol{p}},n^b_{1,\boldsymbol{p}},n^b_{2,\boldsymbol{p}}}(\boldsymbol{\lambda},\boldsymbol{p}) \, |n^a_{1,\boldsymbol{p}}, n^a_{2,\boldsymbol{p}}, n^b_{1,\boldsymbol{p}}, n^b_{2,\boldsymbol{p}}\rangle \right), \tag{2.15}$$

where we have expressed the state in the occupational basis

$$|n^a_{1,\boldsymbol{p}}, n^a_{2,\boldsymbol{p}}, n^b_{1,\boldsymbol{p}}, n^b_{2,\boldsymbol{p}}\rangle = \left(a^\dagger_{1,\boldsymbol{p}}\right)^{n^a_{1,\boldsymbol{p}}} \left(a^\dagger_{2,\boldsymbol{p}}\right)^{n^a_{2,\boldsymbol{p}}} \left(b^\dagger_{1,\boldsymbol{p}}\right)^{n^b_{1,\boldsymbol{p}}} \left(b^\dagger_{2,\boldsymbol{p}}\right)^{n^b_{1,\boldsymbol{p}}} |0000\rangle \, . \tag{2.16}$$

Here $\{n^j_{i,\boldsymbol{p}}\} = 0, 1$ are the fermionic occupation numbers and $|0000\rangle$ is the fermionic vacuum. The eigenstates of (2.1) will be of the form (2.15) with the further condition of normalisation, i.e. $\sum_{n^j_{i,\boldsymbol{p}}=0,1} \left|\alpha_{n^a_{1,\boldsymbol{p}},n^a_{2,\boldsymbol{p}},n^b_{1,\boldsymbol{p}},n^b_{2,\boldsymbol{p}}}(\boldsymbol{\lambda},\boldsymbol{p})\right|^2 = 1$.

As stated previously, we restrict the system to a fixed particle number, i.e. $\left[H, N\right] = 0$ where $N = \sum_{\boldsymbol{p},\alpha=1,2} \left(a^\dagger_{\alpha,\boldsymbol{p}} a_{\alpha,\boldsymbol{p}} + b^\dagger_{\alpha,\boldsymbol{p}} b_{\alpha,\boldsymbol{p}}\right)$. Furthermore, we fix the system to be at half filling, which means that the ground state $|\psi_{\boldsymbol{p}}\rangle$ satisfies the condition $\sum_{i,j} n^j_{i,\boldsymbol{p}} = 2$. This restriction means that a complete local basis for each momentum component of the ground state is given by

$$\left\{ |1100\rangle \, , |1010\rangle \, , |1001\rangle \, , |0110\rangle \, , |0101\rangle \, , |0011\rangle \, \right\}. \tag{2.17}$$

Now we can divide the ground state into two orthogonal subspaces

$$\begin{aligned} |\psi_{\boldsymbol{p}}\rangle =& A \Big| \sum_{i=1,2} n^a_{i,\boldsymbol{p}} : \text{even}; \sum_{i=1,2} n^b_{i,\boldsymbol{p}} : \text{even} \Big\rangle + B \Big| \sum_{i=1,2} n^a_{i,\boldsymbol{p}} : \text{odd}; \sum_{i=1,2} n^b_{i,\boldsymbol{p}} : \text{odd} \Big\rangle \\ \equiv& A \, |e;e\rangle + B \, |o;o\rangle \, , \end{aligned} \tag{2.18}$$

where $\sum_{i=1,2} n^j_{i,\boldsymbol{p}}$ are either both even or both odd and $|A|^2 + |B|^2 = 1$. The next step is to perform a Schmidt decomposition on each part of the state, $|e;e\rangle$ and $|o;o\rangle$, which can be written

$$\begin{aligned} |e;e\rangle =& \cos\theta_e \, |a_e\rangle \otimes |b_e\rangle + \sin\theta_e \, |\tilde{a}_e\rangle \otimes |\tilde{b}_e\rangle \, , \\ |o;o\rangle =& \cos\theta_o \, |a_o\rangle \otimes |b_o\rangle + \sin\theta_o \, |\tilde{a}_o\rangle \otimes |\tilde{b}_o\rangle \, , \end{aligned} \tag{2.19}$$

where $\theta_e, \theta_o \in [0, \pi/2)$ ensuring that the Schmidt coefficients are non-negative. We stipulate that the states $|a_{e/o}\rangle\,|b_{e/o}\rangle$ are written in the same basis as (2.16). The states in (2.19) obey the orthogonality conditions $\langle a_{e/o}|\tilde{a}_{e/o}\rangle = 0$ and $\langle b_{e/o}|\tilde{b}_{e/o}\rangle = 0$. More explicitly we have

$$\begin{aligned} |a_o\rangle &= \left(\alpha_{01} a^\dagger_{2,\boldsymbol{p}} + \alpha_{10} a^\dagger_{1,\boldsymbol{p}}\right)|00\rangle\,, & |\tilde{a}_o\rangle &= \left(\alpha^*_{10} a^\dagger_{2,\boldsymbol{p}} - \alpha^*_{01} a^\dagger_{1,\boldsymbol{p}}\right)|00\rangle\,, \\ |b_o\rangle &= \left(\beta_{01} b^\dagger_{2,\boldsymbol{p}} + \beta_{10} b^\dagger_{1,\boldsymbol{p}}\right)|00\rangle\,, & |\tilde{b}_o\rangle &= \left(\beta^*_{10} b^\dagger_{2,\boldsymbol{p}} - \beta^*_{01} b^\dagger_{1,\boldsymbol{p}}\right)|00\rangle \end{aligned} \tag{2.20}$$

and

$$\begin{aligned} |a_e\rangle &= e^{i\phi_a}\,|00\rangle\,, & |\tilde{a}_e\rangle &= e^{i\tilde{\phi}_a} a^\dagger_{1,\boldsymbol{p}} a^\dagger_{2,\boldsymbol{p}}\,|00\rangle\,, \\ |b_e\rangle &= e^{i\phi_b} b^\dagger_{1,\boldsymbol{p}} b^\dagger_{2,\boldsymbol{p}}\,|00\rangle\,, & |\tilde{b}_e\rangle &= e^{i\tilde{\phi}_b}\,|00\rangle\,, \end{aligned} \tag{2.21}$$

where $|\alpha_{01}|^2 + |\alpha_{10}|^2 = |\beta_{01}|^2 + |\beta_{10}|^2 = 1$. The phases $\phi_{a/b}$ and $\tilde{\phi}_{a/b}$ are in general non-zero however, after multiplying $|\psi_{\boldsymbol{p}}\rangle$ by a global phase of $e^{-i(\phi_a+\phi_b)}$, we can transfer them to the $|o;o\rangle$ subspace via a $U(1)$ local gauge transformation given by

$$a^\dagger_{1,\boldsymbol{p}} \to e^{-i(\tilde{\phi}_a+\tilde{\phi}_b-\phi_a-\phi_b)} a^\dagger_{1,\boldsymbol{p}}. \tag{2.22}$$

After this transformation the only momentum dependence in the $|e;e\rangle$ subspace is in the real and positive Schmidt coefficients $\cos\theta_e$ and $\sin\theta_e$. Having preparaed the state we can now write $\nu_{2\mathrm{D}}(\boldsymbol{\lambda})$

$$\nu_{2\mathrm{D}}(\boldsymbol{\lambda}) = -\frac{i}{2\pi}\oint_{\partial BZ} A^2\,\langle e;e|\boldsymbol{\partial}|e;e\rangle\cdot d\boldsymbol{p} - \frac{i}{2\pi}\oint_{\partial BZ} B^2\,\langle o;o|\boldsymbol{\partial}|o;o\rangle\cdot d\boldsymbol{p} \tag{2.23}$$

where terms containing $A\boldsymbol{\partial}A$ or $B\boldsymbol{\partial}B$ do not contribute because $A\boldsymbol{\partial}A + B\boldsymbol{\partial}B = \boldsymbol{\partial}(A^2+B^2)/2 = 0$ which follows from the reality condition on A and B. Direct evaluation of the integrand in the $|e;e\rangle$ case finds it to be zero because $\cos\theta_e\boldsymbol{\partial}\cos\theta_e + \sin\theta_e\boldsymbol{\partial}\sin\theta_e = \boldsymbol{\partial}(\cos^2\theta_e + \sin^2\theta_e)/2 = 0$. Noting that $\langle i_o|\boldsymbol{\partial}|i_o\rangle =$

$-\langle\tilde{i}_o|\boldsymbol{\partial}|\tilde{i}_o\rangle$ and using the positivity and normalisation of the Schmidt coefficients, a direct evaluation gives

$$\nu_{2\mathrm{D}}(\boldsymbol{\lambda}) = -\frac{i}{2\pi}\sum_{i=a,b}\oint_{\partial BZ} S\,\langle i_o|\boldsymbol{\partial}|i_o\rangle\cdot d\boldsymbol{p}, \quad S = |B|^2T, \tag{2.24}$$

where $T = \cos^2\theta_o - \sin^2\theta_o$ is a measure of the entanglement between the a and b subsystems.

The Chern number is now written as a sum of exclusive contributions from each subsystem. If $S = 1$ then (2.24) is simply a sum of Berry phases associated with each subsystem which can, by (2.12), be written as a sum of winding numbers of a pair of vectors $\hat{\boldsymbol{s}}_a(\boldsymbol{\lambda},\boldsymbol{p})$ and $\hat{\boldsymbol{s}}_b(\boldsymbol{\lambda},\boldsymbol{p})$. However as we shall see that the decomposition only fails when $S \to 0$, when the subsystems are maximally entangled. In section 2.3 we present examples that show that the method only diverges from the theoretical values when $T \to 0$.

2.2.2 Subsystem winding numbers as physical observables

We will now construct the subsystem winding numbers as a function of two vectors $\hat{\boldsymbol{s}}_a(\boldsymbol{\lambda},\boldsymbol{p})$ and $\hat{\boldsymbol{s}}_b(\boldsymbol{\lambda},\boldsymbol{p})$, which are themselves given in terms of the expectation values of the ground state, $|\psi_{\boldsymbol{p}}\rangle$, with some set of observable operators associated with each subsystem. In analogy with (2.14) we can construct the observables associated with the a and b subsystems, $\boldsymbol{\Sigma}_a = \left(\Sigma_a^x,\ \Sigma_a^y,\ \Sigma_a^z\right)$ and $\boldsymbol{\Sigma}_b = \left(\Sigma_b^x,\ \Sigma_b^y,\ \Sigma_b^z\right)$, and they are given explicitly by

$$\begin{aligned}
\Sigma_a^x &= a^\dagger_{1,\boldsymbol{p}}a_{2,\boldsymbol{p}} + a^\dagger_{2,\boldsymbol{p}}a_{1,\boldsymbol{p}} & \Sigma_b^x &= b^\dagger_{1,\boldsymbol{p}}b_{2,\boldsymbol{p}} + b^\dagger_{2,\boldsymbol{p}}b_{1,\boldsymbol{p}}\\
\Sigma_a^y &= -ia^\dagger_{1,\boldsymbol{p}}a_{2,\boldsymbol{p}} + ia^\dagger_{2,\boldsymbol{p}}a_{1,\boldsymbol{p}} & \Sigma_b^y &= -ib^\dagger_{1,\boldsymbol{p}}b_{2,\boldsymbol{p}} + ib^\dagger_{2,\boldsymbol{p}}b_{1,\boldsymbol{p}}\\
\Sigma_a^z &= a^\dagger_{1,\boldsymbol{p}}a_{1,\boldsymbol{p}} - a^\dagger_{2,\boldsymbol{p}}a_{2,\boldsymbol{p}} & \Sigma_b^z &= b^\dagger_{1,\boldsymbol{p}}b_{1,\boldsymbol{p}} - b^\dagger_{2,\boldsymbol{p}}b_{2,\boldsymbol{p}}
\end{aligned} \tag{2.25}$$

Now we can calculate the expectation values

$$\langle\psi_{\boldsymbol{p}}|\boldsymbol{\Sigma}_i|\psi_{\boldsymbol{p}}\rangle = |A|^2\,\langle e;e|\boldsymbol{\Sigma}_i|e;e\rangle + |B|^2\,\langle o;o|\boldsymbol{\Sigma}_i|o;o\rangle \tag{2.26}$$

where cross terms between the even and odd subspaces do not appear since the operators given in (2.25) conserve particle number. By direct evaluation of the $|e;e\rangle$ term we see that it vanishes. Evaluation of the $|o;o\rangle$ term gives

$$\langle o;o|\boldsymbol{\Sigma}_i|o;o\rangle = \cos^2\theta_o\,\langle i_o|\boldsymbol{\Sigma}_i|i_o\rangle + \sin^2\theta_o\,\langle\tilde{i}_o|\boldsymbol{\Sigma}_i|\tilde{i}_o\rangle = T\,\langle i_o|\boldsymbol{\Sigma}_i|i_o\rangle \tag{2.27}$$

where we have used the tracelessness of the $\boldsymbol{\Sigma}_i$ operators which implies $\langle\tilde{i}_o|\boldsymbol{\Sigma}_i|\tilde{i}_o\rangle = -\langle i_o|\boldsymbol{\Sigma}_i|i_o\rangle$. Each case is explicitly given by

$$\begin{aligned}\langle\psi_{\boldsymbol{p}}|\boldsymbol{\Sigma}_a|\psi_{\boldsymbol{p}}\rangle &= S\,\langle\psi_a(\boldsymbol{p})|\boldsymbol{\sigma}|\psi_a(\boldsymbol{p})\rangle \\ \langle\psi_{\boldsymbol{p}}|\boldsymbol{\Sigma}_b|\psi_{\boldsymbol{p}}\rangle &= S\,\langle\psi_b(\boldsymbol{p})|\boldsymbol{\sigma}|\psi_b(\boldsymbol{p})\rangle\,,\end{aligned} \tag{2.28}$$

where $|\psi_a(\boldsymbol{p})\rangle = \begin{pmatrix}\alpha_{01} & \alpha_{10}\end{pmatrix}^{\mathrm{T}}$ and $|\psi_b(\boldsymbol{p})\rangle = \begin{pmatrix}\beta_{01} & \beta_{10}\end{pmatrix}^{\mathrm{T}}$. We can normalise the vectors given in (2.28) and relabel them as

$$\hat{\boldsymbol{s}}_i(\boldsymbol{p}) = \frac{\boldsymbol{s}_i(\boldsymbol{p})}{|\boldsymbol{s}_i(\boldsymbol{p})|} = \langle\psi_i(\boldsymbol{p})|\boldsymbol{\sigma}|\psi_i(\boldsymbol{p})\rangle\,, \tag{2.29}$$

where $|\boldsymbol{s}_i(\boldsymbol{p})| = |B|^2|T|^2$. In much the same way as presented in 2.1 we can define subsystem Chern numbers for the $|i_o\rangle$ states as Berry phases

$$\nu^i_{2\mathrm{D}} = -\frac{i}{2\pi}\oint_{\partial\mathrm{BZ}}\langle i_o|\boldsymbol{\partial}|i_o\rangle\cdot d\boldsymbol{p} \tag{2.30}$$

or as subsystem winding numbers

$$\nu^i_{2\mathrm{D}} = \frac{1}{4\pi}\int_{\mathrm{BZ}} d^2p\;\;\hat{\boldsymbol{s}}_i(\boldsymbol{p})\cdot\left(\partial_{p_x}\hat{\boldsymbol{s}}_i(\boldsymbol{p})\times\partial_{p_y}\hat{\boldsymbol{s}}_i(\boldsymbol{p})\right) \tag{2.31}$$

We can view $|\psi_i(\boldsymbol{p})\rangle$ as the ground state of some fictitious kernel Hamiltonian $h_i(\boldsymbol{\lambda},\boldsymbol{p}) = \hat{\boldsymbol{s}}_i(\boldsymbol{p})\cdot\boldsymbol{\sigma}$. We have shown that each subsystem Berry phase (2.30) is proportional to its corresponding subsystem winding number (2.31) and that the winding numbers are physically observable. We now show that, with slight modifications, the above method applies to topological superconductors that conserve particle parity.

2.2.3 Derivation for superconductors

Again we take the Hamiltonian of the system to be (2.1), but now the spinor takes the form $\boldsymbol{\psi}_{\boldsymbol{p}} = \begin{pmatrix} a_{\boldsymbol{p}} & a^\dagger_{-\boldsymbol{p}} & b_{\boldsymbol{p}} & b^\dagger_{-\boldsymbol{p}} \end{pmatrix}^{\mathrm{T}}$. A general state in the Hilbert space can be written as in (2.15) but with the Fock space ordered as

$$|n^a_{\boldsymbol{p}}, n^a_{-\boldsymbol{p}}, n^b_{\boldsymbol{p}}, n^b_{-\boldsymbol{p}}\rangle = \left(a^\dagger_{\boldsymbol{p}}\right)^{n^a_{\boldsymbol{p}}} \left(a^\dagger_{-\boldsymbol{p}}\right)^{n^a_{-\boldsymbol{p}}} \left(b^\dagger_{\boldsymbol{p}}\right)^{n^b_{\boldsymbol{p}}} \left(b^\dagger_{-\boldsymbol{p}}\right)^{n^b_{-\boldsymbol{p}}} |0000\rangle \tag{2.32}$$

Superconductors only preserve total parity, i.e. $\left[H, P\right] = 0$ with $P = \exp\Big(i\pi \sum_{\boldsymbol{p}} \left(a^\dagger_{\boldsymbol{p}} a_{\boldsymbol{p}} + b^\dagger_{\boldsymbol{p}} b_{\boldsymbol{p}}\right)\Big) = P_a P_b$, while subsystem parities, P_a and P_b, are not independently conserved. Without loss of generality we assume that the ground state is in the total even parity sector. This means that the subsystems are correlated such that $P_a = P_b$, which in turn means that the ground state complies with the condition of overall momentum. Under these conditions the ground state is given in the basis spanned by the states

$$\left\{ |0000\rangle, |0011\rangle, |1100\rangle, |1111\rangle, |0110\rangle, |1001\rangle \right\}. \tag{2.33}$$

As in the insulating case we divide the ground state into even and odd subspaces

$$|\psi_{\boldsymbol{p}}\rangle = A\,|e;e\rangle + B\,|o;o\rangle\,. \tag{2.34}$$

Performing the Schmidt decomposition between the a and b subspaces in this parity sector we obtain a general expression which has the same form as (2.19) but with the Schmidt bases given by

$$\begin{aligned} |a_e\rangle &= \left(\alpha_{00} + \alpha_{11} a^\dagger_{\boldsymbol{p}} a^\dagger_{-\boldsymbol{p}}\right)|00\rangle\,, & |\tilde{a}_e\rangle &= \left(\alpha^*_{11} - \alpha^*_{00} a^\dagger_{\boldsymbol{p}} a^\dagger_{-\boldsymbol{p}}\right)|00\rangle\,, \\ |b_e\rangle &= \left(\beta_{00} + \beta_{11} b^\dagger_{\boldsymbol{p}} b^\dagger_{-\boldsymbol{p}}\right)|00\rangle\,, & |\tilde{b}_e\rangle &= \left(\beta^*_{11} - \beta^*_{00} b^\dagger_{\boldsymbol{p}} b^\dagger_{-\boldsymbol{p}}\right)|00\rangle\,, \end{aligned} \tag{2.35}$$

and

$$|a_o\rangle = e^{i\phi_a} a^\dagger_{-\boldsymbol{p}} |00\rangle\,, \qquad |\tilde{a}_o\rangle = e^{i\tilde{\phi}_a} a^\dagger_{\boldsymbol{p}} |00\rangle\,,$$
$$|b_o\rangle = e^{i\phi_b} b^\dagger_{\boldsymbol{p}} |00\rangle\,, \qquad |\tilde{b}_o\rangle = e^{i\tilde{\phi}_b} b^\dagger_{-\boldsymbol{p}} |00\rangle\,. \tag{2.36}$$

In a similar way to the insulating case, all coefficients except those in the $|o;o\rangle$ subspace can be made real via $U(1)$ guage transformations. With this in mind, the decomposition of the Berry phase proceeds in the same way as the insulating case with the only difference being that the contribution from the $|o;o\rangle$ subspace vanishes and we are left with

$$\nu_{\mathrm{2D}}(\boldsymbol{\lambda}) = -\frac{i}{2\pi} \sum_{i=a,b} \oint_{\partial BZ} S \,\langle i_o|\boldsymbol{\partial}|i_o\rangle \cdot d\boldsymbol{p}, \quad S = |A|^2 T. \tag{2.37}$$

The observable operators, $\boldsymbol{\Sigma}_i$, used to evaluate the subsystem winding nubmers are now given by

$$\Sigma^x_a = a^\dagger_{\boldsymbol{p}} a^\dagger_{-\boldsymbol{p}} + a_{-\boldsymbol{p}} a_{\boldsymbol{p}}, \qquad \Sigma^x_b = b^\dagger_{\boldsymbol{p}} b^\dagger_{-\boldsymbol{p}} + b_{-\boldsymbol{p}} b_{\boldsymbol{p}},$$
$$\Sigma^y_a = -ia^\dagger_{\boldsymbol{p}} a^\dagger_{-\boldsymbol{p}} + ia_{-\boldsymbol{p}} a_{\boldsymbol{p}}, \qquad \Sigma^x_b = -ib^\dagger_{\boldsymbol{p}} b^\dagger_{-\boldsymbol{p}} + ib_{-\boldsymbol{p}} b_{\boldsymbol{p}},$$
$$\Sigma^z_a = a^\dagger_{\boldsymbol{p}} a_{\boldsymbol{p}} - a^\dagger_{-\boldsymbol{p}} a_{-\boldsymbol{p}}, \qquad \Sigma^z_b = b^\dagger_{\boldsymbol{p}} b_{\boldsymbol{p}} - b^\dagger_{-\boldsymbol{p}} b_{-\boldsymbol{p}}. \tag{2.38}$$

2.3 Examples

2.4 Experimental applications

2.5 Conclusions

Bibliography

[1] A. Y. Kitaev, Physics-Uspekhi **44**, 131 (2001). 1

[2] S. Ryu, A. P. Schnyder, A. Furusaki, and A. W. W. Ludwig, New Journal of Physics **12**, 065010 (2010). 3

[3] X.-G. Wen, Phys. Rev. B **85**, 085103 (2012). 3

[4] A. P. Schnyder, S. Ryu, A. Furusaki, and A. W. W. Ludwig, Phys. Rev. B **78**, 195125 (2008). 3

[5] J. de Lisle *et al.*, New Journal of Physics **16**, 083022 (2014). 8